Journal of Research in Pharmacy

Research Article

www.jrespharm.com

Response surface methodology for optimization of turmeric essential oil-loaded nanoemulgel

Nining NINING [1] *, Anisa AMALIA [1], Fatimatuz ZAHROK [2]

[1] Department of Pharmaceutical Technology, Faculty of Pharmacy and Science, Universitas Muhammadiyah Prof. DR. Hamka, Jakarta, Indonesia.

[2] Department of Pharmacy, Faculty of Pharmacy and Science, Universitas Muhammadiyah Prof. DR. Hamka, Jakarta, Indonesia.

* Corresponding Author. E-mail: nining@uhamka.ac.id (N.N.); Tel. +62-81224042122.

Received: 03 September 2022 / Revised: 06 March 2023 / Accepted: 09 March 2023

ABSTRACT: Turmeric Essential Oil (TEO) has an antioxidant and anti-inflammatory activity to be formulated in a topical dosage form. Nanoemulgels (Negs) development, based on varying concentrations of emulsifiers and gel formers, affects their characteristics and stability. This study focuses on optimizing TEO-loaded Negs based on physical and mechanical characterization, which have promising topical applications. Negs were created using the high-energy approach and optimized using Response Surface Methodology (RSM) and the Central-Composite Design (CCD) for the optimization of span-80/tween-80 (X_1) and Carbopol® 980. (X_2). Observed variable responses were particle size (PS) (Y_1), polydispersity index (PDI) (Y_2), zeta potential (ZP) (Y_3), pH (Y4), spreadability (Y_5), and adhesion time (AT) (Y_6). Actual responses of Negs were compared with the CCD-RSM predictions to validate the model. In addition, other physical evaluations were observed, such as organoleptic observations, homogeneity, freeze-thaw tests, viscosity, and flow properties. Optimized TEO-loaded Negs were made with 8.68% span-80/tween-80 and 1.18% Carbopol® 980. The evaluation results showed the optimal TEO-loaded Negs on nano-metric size (182.3 ± 5.5 nm) with low PDI (0.242 ± 0.003), good ZP (-57.23 ± 2.91 mV), pH (4.51 ± 0.02), spreadability (6.0 ± 0.2 cm), and AT (6.45 ± 0.19 s). TEO-loaded Negs have an excellent appearance and did not run phase separation at extreme temperature storage with pseudoplastic thixotropy flow. Thus, the developed TEO-loaded Negs can be a potential delivery system and a promising suitable approach for topical preparations.

KEYWORDS: Central composite design; nanoemulgels; response surface methodology; turmeric essential oil; topical delivery.

1. INTRODUCTION

Turmeric is the dried rhizome of *Curcuma longa* L. (Zingiberaceae), which derives from Southeast Asia and is cultivated mainly in India, followed by Bangladesh, China, Thailand, Cambodia, Indonesia, Malaysia, and the Philippines [1]. Steam distillation extracts turmeric essential oil (TEO) from the turmeric rhizome [2]. Chemical constituents with the most significant proportion were oxygenated monoterpenes and sesquiterpenes, which include β-turmerone, α-turmerone, and ar-turmerone [3-5]. The pharmacological activities of TEO have been reported in the form of antioxidants, anti-inflammatory, antinociceptive, antidermatophytic, antifungal, and antibacterial activities [2,6–9]. These reducing power and radical scavenging abilities are associated with the high antioxidant potential of TEO [8,10]. This pharmacological activity justifies its use in various applications, including cosmetics and phytomedicines [7,11,12]. Like other essential oil, TEO has limited use due to its volatility, instability under certain conditions, lipophilicity, and low aqueous solubility [13,14]. Many recent studies are oriented toward solving these limitations, so that efficacy of the essential oil lasts longer and increases.

Previously, TEO has been developed for cream as a conventional drug delivery system, patch, and nanoemulsions [7,11,15,16]. Most water-based liquid or semisolid systems have limitations in delivering lipophilic drugs [17]. Nanoemulsions are an established alternative for delivering lipophilic drugs by increasing topical absorption [18]. The main advantage of topically administered nanoemulsions is the ability to increase penetration and permeation of drugs through the skin without adding non-physical enhancers and a large number of surfactants to the formulation, which can cause skin irritation, especially with long-term usage [18,19]. However, this system has problems with low viscosity due to poor spreadability and skin

How to cite this article: Nining N, Amalia , Zahrok F. Response surface methodology for optimization of turmeric essential oil-loaded nanoemulgel. J Res Pharm. 2023; 27(4): 1499-1512.

https://doi.org/10.12991/jrp.2019.00

ISSN: 2630-6344

retention [20]. Nanoemulgels (Negs), a combination of nanoemulsion and hydrogel, were made to improve the characteristics [18,19,21].

Negs consist of a hydrogel system and an emulsion with nano-sized globules. An emulsifier in the form of surfactants and co-surfactants stabilizes the emulsion, which serves as a drug delivery platform [18][. Surfactants reduce the interfacial surface tension of immiscible liquids and change the entropy of the dispersion, thereby stabilizing a thermodynamically unstable system; co-surfactants are combined with surfactants in the emulsification process by disrupting the surface layer [22]. The emulsifier plays a role in the emulsification process to increase stability when the product is kept for an extended time. On the other side, gels are made from polymers, a gel former, that expand after absorbing a liquid [23]. Gel former increase the viscosity of the formulation and can react with emulsifiers to change the thickness [24]. In addition, topical Negs can increase patient compliance because of their non-irritating, non-greasy characteristics and improved drug release [25]. However, the available methods for manufacturing Negs exhibit various limitations, which directly or indirectly affect the quality of the Negs formulations.

Currently, the principle of quality by design is adopted to ensure the quality of drugs, their safety, and efficacy [26]. The quality by design (QbD) trend is used to develop, optimize, and investigate the interaction between particular variables and their related responses to achieve the optimal formulation [27]. Our study used Central Composite Design (CCD) on Response Surface Methodology (RSM) to select optimal formulations and predict models that rely on statistical analysis (ANOVA) and exact equations [28,29]. In this aspect, we intended to develop a TEO-loaded Negs that would be optimized using a complete 2^2-factorial design and determine the independent factors' precise influence on the investigated dependent variables. The choice and procedure factors were span-80/tween-80 (X_1) and Carbopol® 980 (X_2). Response variables investigated were particle size (PS) (Y1), polydispersity index (PDI) (Y2), zeta potential (ZP) (Y3), pH (Y4), spreadability (Y5), and adhesion time AT) (Y6). This work is the first step in developing an optimized TEO preparation suitable for transdermal drug delivery for topical application.

2. RESULTS AND DISCUSSION

2.1. Identification of TEO

TEO identification is carried out to ensure the quality of the active ingredients. The tests included organoleptic, phytochemical identity in the form of phenolics and terpenoids, and antioxidant activity by the DPPH method. The results of this study can be seen in **Figure 1**. Organoleptically, TEO is an orange liquid with a distinctive turmeric aroma. Identification results in the phenolic test showed a black-green color (**Figure 1A**) due to the formation of a phenolic-Fe^{3+} complex [30]. In the terpenoid test, reaction results show a purple color (**Figure 1B**) as a positive sign. Based on these results, it can be concluded that TEO contains phenolic and terpenoid compounds. Several studies reported that TEO has powerful antioxidant potential both *in-vitro* and *in-vivo* [2,8,31]. Oxygenated monoterpenes and sesquiterpenes, such as ar-turmerone, α-turmerone, and β-turmerone, were included in the terpenoid compounds and reported to play a role in this activity. In addition, contained phenol was also reported to perform as an excellent free radical scavenger because its reduction potential was lower than oxygen's [8]. In our study, the antioxidant activity of TEO was presented as an IC_{50} of 9.88 µm/ml, which was included in the powerful antioxidant category because of below 50 µm/ml [32]. It differed from other studies' results, which showed an IC_{50} of 2274.02 µm/ml and above 1000 µm/ml [2,10]. Meanwhile, similar findings stated IC_{50} values of 10.03 µm/ml, 3.227 µm/ml, and 14.5 µm/ml [33–35]. The difference value was due to the use of TEO from different origin sources, regional conditions, and the extraction method used.

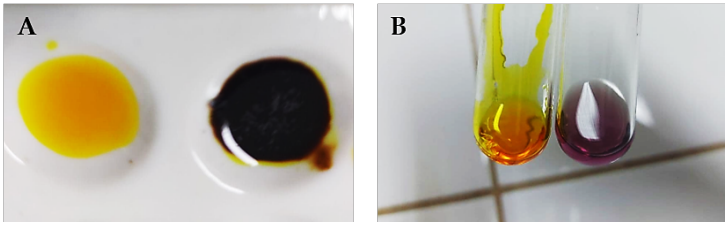

Figure 1. The result of qualitative test observation is a phenolic test with a positive result marked in a blackish green color (a) and a terpenoid test with a positive result marked with a purple color (b).

2.2. Preparation of TEO-loaded Negs

TEO-loaded Negs were produced using the high-energy method efficiently. A high-pressure homogenizer provides sufficient energy to increase the interfacial area and generate nano-size globules [36]. An emulsion system with a nanodroplet size must have flow properties that allow it to pass through the homogenizer [37]. Flow properties are inversely correlated with the amount of emulsifier and gel former added to the Negs formulation. In this study, the selected optimized formulation was the one that produces Negs with the smallest size, as shown by the limitations in **Table 3**. Therefore, the range of regulated emulsifiers and gel formers concentrations still provides flow properties that allow the flow to remain good using a high-energy homogenizer. In general, the preparation of Negs was carried out in 3-stages, namely, nanoemulsions preparation, gel preparation, and Negs preparation. Negs were successfully produced in 14-formulation with variations of emulsifiers and gel former with compositions that can be seen in **Table 1**.

Tabel 1. Evaluation results of independent variables and dependent variables with the CCD design for optimizing TEO-loaded Negs.

Std	X_1 (%)	X_2 (%)	Y_1 (nm)	Y_2	Y_3 (mV)	Y_4	Y_5 (cm)	Y_6 (s)
1	5.50	1.02	206.9 ± 0.7	0.571 ± 0.000	35.39 ± 1.50	5.45	5.55	5.65
2	2.32	1.15	457.0 ± 0.9	0.000 ± 0.000	13.90 ± 1.92	4.60	5.00	6.99
3	8.68	0.90	166.7 ± 0.4	0.378 ± 0.074	31.64 ± 0.53	6.35	6.20	4.23
4	2.32	0.90	411.0 ± 5.8	0.000 ± 0.000	30.67 ± 0.89	6.29	5.00	4.30
5	5.50	1.02	302.1 ± 3.6	0.571 ± 0.000	36.45 ± 0.45	5.46	5.60	5.63
6	5.50	1.02	263.0 ± 3.7	0.571 ± 0.000	18.49 ± 1.77	5.47	5.55	5.64
7	8.68	1.15	198.1 ± 1.2	0.242 ± 0.003	57.23 ± 2.91	4.65	6.15	6.95
8	5.50	1.02	246.9 ± 7.2	0.571 ± 0.000	26.60 ± 0.17	5.46	5.60	5.67
9	5.50	1.02	206.0 ± 2.3	0.571 ± 0.000	31.77 ± 1.01	5.46	5.60	5.65
10	10.00	1.02	160.8 ± 1.3	0.285 ± 0.024	46.72 ± 1.97	5.31	6.25	5.84
11	1.00	1.02	244.2 ± 4.3	0.571 ± 0.000	31.26 ± 0.57	5.78	4.90	6.88
12	5.50	1.02	238.1 ± 3.0	0.571 ± 0.000	30.78 ± 0.53	5.45	5.55	5.64
13	5.50	1.20	206.2 ± 1.6	0.571 ± 0.000	30.56 ± 0.78	4.57	5.50	7.08
14	5.50	0.85	240.5 ± 2.2	0.571 ± 0.000	20.12 ± 0.16	6.39	5.65	4.22

Y_1: Particle size (PS), Y_2: Polydispersity index (PDI), Y_3: Zeta potensial (ZP), Y_4: pH, Y_5: Spreadability, Y_6: Adhesion time (AT)

2.3. Experimental Design by CCD-RSM

2.3.1. Fitting the Model

TEO-loaded Negs were optimized based on CCD in the RSM. CCD was used to establish the optimal concentrations of emulsifier (X_1) and gel former (X_2) as the key parameters influencing the dependent response. Prediction of the factorial axial design and the possible curvature in the response could be obtained from the optimization process with an effective second-level design [38]. Predicting the significant influence of the independent variable on the dependent variable is essential for generating TEO-loaded Negs. Based on the literature survey, two factors were chosen as independent variables, and six responses were chosen as the dependent variable with the most significant influence on Negs. The independent variables with their levels and the observed response variables are presented in **Table 1**.

2.3.2. Analysis of Design

Statistical data analysis must be carried out to predict and recognize the model. **Table 2** shows the statistical analysis of a quadratic model for PDI, a 2FI model for ZP, and linear models for PS, pH, AT, and spreadability. This table identifies factors with p-values less than a predefined threshold (0.01 and 0.05, with a 99% and 95% confidence level, respectively) as influential factors. Besides the significant p-value, a large F-value minimizes error in the model and lack of fit, preferably non-significant to fit the model data [27,39]. Depending on the most significant R-squared value and the least residual predictive sum of squares value, the six responses demonstrated distinct models in their application. The chosen model had a non-statistically significant lack of fit, and model validation was confirmed by the residual plot test of the regression model, which was supported by supplemental information for all responses. Compared to the 2FI and simple linear models, the quadratic model represented the impacts of numerous variables, including individual factors, interactions, and the quadratic influence on the response.

Table 2. Statistical analysis of PS (Y_1), PDI (Y_2), ZP (Y_3), pH (Y_4), spreadability (Y_5), and AT (Y_6) TEO-loaded Negs on CCD.

Factors		Y_1	Y_2	Y_3	Y_4	Y_5	Y_6
X_1	Coefficient	-77.64	0.027	8.27	-0.069	0.53	-0.20
	p-value	0.0063**	0.7325	0.0080**	0.1430	<0.0001**	0.1406
X_2	Coefficient	3.61	-0.017	2.95	-0.75	-0.033	1.18
	p-value	0.8783	0.8289	0.2668	<0.0001**	0.1157	<0.0001**
X_1X_2	Coefficient		-0.034	10.59			
	p-value		0.7602	0.0136*			
X_1^2	Coefficient		-0.16				
	p-value		0.0818				
X_2^2	Coefficient		-0.086				
	p-value		0.3087				
Intercept	Coefficient	253.39	0.57	31.54	5.48	5.58	5.74
Degree of freedom		2	5	3	2	2	2
Sum of squares		48332.05	0.24	1065.33	4.48	2.28	11.49
Mean of squares		24166.02	0.047	355.11	2.24	1.14	5.74
F-value		5.69	1.02	7.06	145.08	386.43	46.35
p-value		0.0201	0.4645	0.0078	<0.0001	<0.0001	<0.0001
R-Squared		0.5084	0.3898	0.6794	0.9635	0.9860	0.8939

X_1: span-80/tween-80; X_2: Carbopol® 980
* p-value < 0.05
** p-value < 0.01

2.3.3. Effect of Independent Variables on Dependent Variables

PS parameters are often used to characterize nanoparticles. Negs globule diameter means (Y_1) was adjusted from 160.8 nm (STD#10) to 457.0 nm (STD#2). Based on **Table 2**, the PS response indicates a significantly linear model with an F-value of 5.69 (p-value 0.0201 < 0.05). The suggested linear model equation can be seen as follows:

$$Y_1 = 253.39 - 77.64X_1 + 3.61X_2$$

The equation shows that the Negs PS is significantly (p-value < 0.01) affected by emulsifier concentration (X_1). The positive coefficient has a synergistic effect on the response. In contrast, the negative coefficient has an antagonistic effect which concludes the inverse relationship of the independent variable with a response [38,40]. In addition, this factor has a more significant coefficient. It directly affects the PS, which means that increasing emulsifier concentration causes a decrease in the globule diameter PS in the TEO-loaded Negs. High emulsifier (above 5.5%) resulted in globules measuring below 200 nm, and low emulsifier (below 5.5%) produced globules above 200 nm. This fact is in line with other studies that increasing emulsifiers could reduce droplet Negs PS [41,42]. The emulsifier reduced the interfacial surface tension between the water and oil phases, which decreased the free energy required to disrupt or break the globules and resulted in a smaller droplet diameter. It can also produce a protective cover over the globules, preventing them from coalescence. However, the emulsifier must absorb quickly enough around the droplet to form this protective layer [42,43].

Meanwhile, Carbopol® 980 had no significant effect on PS. The same findings were obtained from the globule size Negs from Carbopol® 934 and 940 as gel former [19]. A response surface plot (**Figure 2A**) may therefore be used to represent the combined influence of variables X_1 and X_2, which shows that Y_1 changes linearly with the sum of the two variables. Nevertheless, the higher gradient in the response surface with span-80/tween-80 (X_1) – not Carbopol® 980 (X_2) – was evidenced from the comparative plot of the response surface. From this explanation, it can be concluded that the PS can be changed by selecting the right X_1 level.

Journal of Research in Pharmacy
Research Article

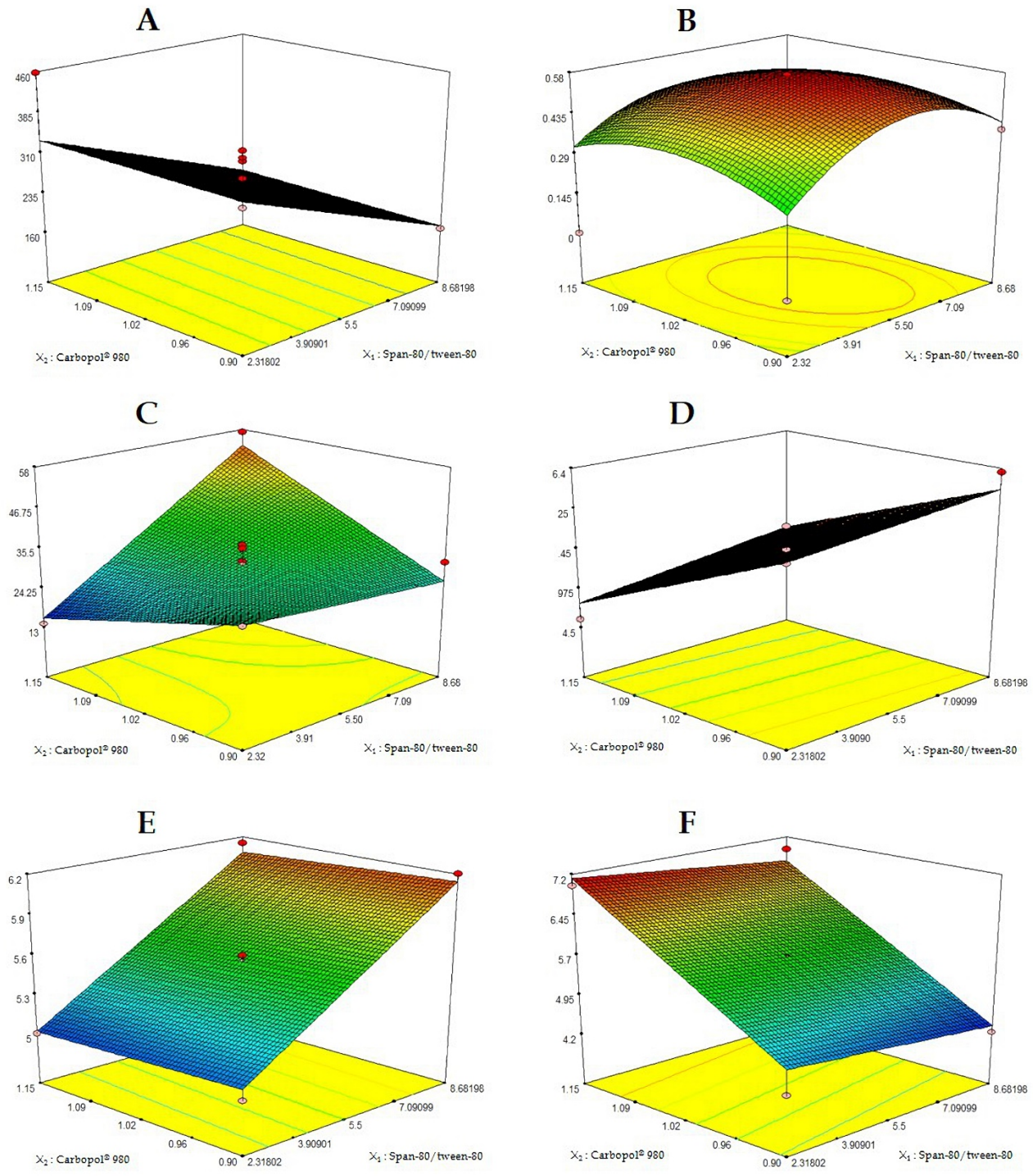

Figure 2. Effect of span-80/tween-80 and Carbopol® 980 concentration on PS (a) PDI (b) ZP (c) pH (d) spreadability (e) AT (f).

In **Table 1**, Negs PDI (Y_2) varied from 0.000 (STD#2 and #4) to 0.571 (STD#1, #5, #6, #8, #9, #11 to #14). PDI measures the distribution of molecular mass in a sample. The smaller PDI (close to 0), the more stable the Negs formulation caused; the large PDI indicates particles formed are not uniform, and the formulation will flocculate quickly. An index value less than 0.05 is included in monodisperse, while an index greater than 0.7 indicates that the sample has a broad PS distribution. A-0.2 and below are considered acceptable for

nanoparticle preparations [44]. Based on **Table 2**, the PDI response shows a non-significant quadratic model with an F-value of 1.02 (p-value 0.4645 > 0.05). Measurements between variables and responses are not a precise cause of that. The suggested quadratic model equation can be seen as follows:

$$Y_2 = 0.57 + 0.027X_1 - 0.017X_2 - 0.034X_1X_2 - 0.16X_1^2 - 0.086X_2^2$$

The equation and p-value of each factor did not significantly affect PDI. The response surface plot (**Figure 2B**) depicts the combined influence of variables X_1 and X_2, which shows that Y_2 changes with the sum of the two variables by model.

The Negs ZP (Y_3) was in the range of 13.90 mV (STD#2) to 46.72 mV (STD#10) (**Table 1**). ZP represents the electric charge between the shear plane of a final outer layer and bulk solution, which significantly affects dispersion stability [45]. This factor is strongly influenced by the composition of the Negs and its electrical phenomena. TEO-loaded Negs, which have positive ZP, show good interaction with negatively charged skin [46]. ZP is the scientific term for the electrokinetic potential in colloidal systems. The high electric charge on the nanoparticle surface will prevent nanoparticle aggregation because of the strong repulsion between particles. The ZP requirement for stability is above ± 30 mV [19]. The higher ZP and the slower aggregation are formed to prevent separation [47]. Based on **Table 2**, the ZP response indicates a significant 2FI model with an F-value model of 7.06 (p-value 0.0078 < 0.05). The linear model equation suggested by the software can be seen as follows:

$$Y_3 = 31.54 + 8.27X_1 + 2.95X_2 + 10.59X_1X_2$$

The equation shows that the Negs ZP was significantly affected by the emulsifier (X_1) and gel former-emulsifier interaction (X_1X_2). ZP was usually influenced by the physicochemical properties of the drug, polymer, carrier, electrolyte presence, and their adsorption [48]. One study stated that adding Carbopol® only slightly increased the ZP Negs [19]. The response surface plot (**Figure 2C**) depicts the combined influence of variables X_1 and X_2, showing that Y_3 changes with the sum of the two variables. Nevertheless, the higher gradient in the response surface with span-80/tween-80 (X_1) – not Carbopol® 980 (X_2) – is the evidence from the comparative plot of the response surface. This description concludes that the ZP can be changed by selecting the proper X_1 level.

The pH test was carried out to measure Negs's acidity or alkalinity level. The pH values (Y_4) were in the range of 4.57 (STD#13) to 6.39 (STD#14) (**Table 1**). The pH requirement of Negs is the same as the skin pH. Too-acidic preparations can irritate the skin and cause a stinging sensation, while too-alkaline preparations can cause dry and itchy skin. The pH result test on 14 formulations was eligible and compatible with the skin (4.5-6.5) [49]. Based on **Table 2**, a linear model was found to be significant in pH response with a model F-value of 145.08 (p-value < 0.0001). The linear model equation suggested by the software can be seen as follows:

$$Y_4 = 5.48 - 0.069X_1 - 0.75X_2$$

The equation shows that the pH was significantly (p-value < 0.0001) affected by gel former (X_2). Carbopol is a high molecular weight homopolymer and acrylic acid copolymer crosslinked with polyalkenyl polyethers [50]. They are anionic and acidic (2.5–4.0 in 2% dispersion) when not neutralized with bases to achieve a specific viscosity [50,51]. Therefore, adding Carbopol to a formulation with a fixed amount of base (triethanolamine) will significantly lower the pH of Negs. The response surface plot (**Figure 2D**) may then be used to depict the combined influence of variables X_1 and X_2, which shows that Y_4 changes linearly with the sum of the two variables. Nevertheless, the higher gradient in the response surface with Carbopol® 980 (X_2) – not span-80/tween-80 (X_1) – is the evidence from the comparative plot of the response surface. This description concludes that the choice of the X_2 level affects the pH Negs.

Spreadability was measured to ensure comfortable use on the skin because it spreads quickly [24]. Terms of good dispersion are 5-7 cm. If the dispersion is too small, it is relatively difficult to spread when applied to the skin, while the dispersion tends to spread too quickly when applied, so it will cause an uncomfortable feeling when used [52]. Based on the results, only one Neg did not meet the requirements, namely F11. **Table 1** shows the range of spreadability (Y_5) from 4.90 cm (STD#11) to 6.25 cm (STD#10). Based on **Table 2**, the spreadability response indicates a significant linear model with an F-value of 386.43 (p-value <0.0001). The linear model equation suggested by the software can be seen as follows:

$$Y_5 = 5.58 + 0.53X_1 - 0.033X_2$$

The equation shows that the spreadability of Negs was significantly (p-value < 0.0001) positively affected by the emulsifier (X_1). That was also found in other literature studies [24]. The higher the Carbopol-contained Negs, the more viscous Negs. AT and spreadability have the opposite results. The higher the Negs' viscosity, the higher the adhesive strength produced, while the smaller the dispersion power [53]. The response surface plot (**Figure 2E**) depicts the combined influence of variables X_1 and X_2, which shows that Y_5 changes linearly with the sum of the two variables. Nevertheless, the higher gradient in the response surface

with span-80/tween-80 (X_1) – not Carbopol® 980 (X_2) – is the evidence from the comparative plot of the response surface. This description concludes that the scatter can be changed by choosing the right X_1 level.

Topical dosage forms, such as Negs, adhere to the skin in two ways: they adhere directly to the rough surface to form a "mechanical interlock" and to the surface via interaction [54]. Good adhesion to Negs supports a higher concentration gradient towards the skin and provides more drug penetration [18]. Adhesive strength is directly related to the AT on the Negs as measured using the single-lap shear test method with slight modifications [55,56]. The test was carried out by applying a shear load to the plates that flank the sample, which had been pre-loaded, and given a measured force; the time taken for the plates to separate was recorded as AT. In our study, the AT was from 4.22 s (STD#14) to 7.08 s (STD#13) in **Table 1**. They met the requirements based on the AT test results on a 14 formulation. An AT was carried out to see how long a Negs could be attached to the skin. The AT requirement is more than 4 seconds. The longer a Negs could be attached to the skin, it showed the better result, where it is expected that more active substances can be absorbed due to the time the Negs was in contact with the skin [57]. Based on **Table 2**, the linear model was found to be significant in the AT response with an F-value model of 46.35 (p-value < 0.0001). The linear model equation suggested by the software can be seen as follows:

$$Y_6 = 5.74 - 0.20X_1 + 1.18X_2$$

The equation reveals that the AT was significantly (p-value < 0.0001) affected by the gel former (X_2) or, indirectly, the same adhesion strength. This finding is in agreement with the literature [58,59]. A response surface plot (**Figure 2F**) may therefore be used to depict the combined influence of variables X_1 and X_2, which shows that Y_6 changes linearly with the sum of the two variables. Nevertheless, the higher gradient in the response surface with Carbopol® 980 (X_2) – not span-80/tween-80 (X_1) – is the evidence from the comparative plot of the response surface. From this explanation, it can be concluded that the AT can be changed by selecting the right X_2 level. Details of the ANOVA results for measured responses are also presented in **Table 2**. In the end, the emulsifier factor significantly affected the response of PS, ZP, and spreadability of TEO-loaded Negs. At the same time, gel former affects the AT and pH.

2.4. Optimized TEO-loaded Negs

The formulation was optimized with Design-Expert®, version 13 software. The optimized Negs were selected based on the minimum PS and PDI; maximum ZP; value in pH range, spreadability, and AT (**Table 3**). Variables composition for optimized Negs is span-80/tween-80 of 8.68% and Carbopol® 980 of 1.18% with a desirability value of 0.801. The formulation with the maximum desirability value is the optimal formulation generated from the optimization phase of the program [60] —the optimization value formed as indicated by the desirability value close to one.

Table 3. The independent and dependent variables with levels and limits in CCD for TEO-loaded Negs development.

Variables	Code	Start point (-α)	Low level (-1)	Central level	High level (+1)	Start point (+α)	Units
Independent variables							
Span-80/tween-80	X_1	0.85	2.32	1.02	5.50	1.20	% w/w
Carbopol® 980	X_2	1	0.90	5.50	1.02	10	% w/w
Dependent variables		**Limits**					
Particle size (PZ)	Y_1	Minimum					nm
Polydispersity index (PDI)	Y_2	Minimum					
Zeta potensial (ZP)	Y_3	Maximum					mV
pH	Y_4	is in range					
Spreadability	Y_5	is in range					cm
Adhesion time (AT)	Y_6	is in range					s

The desirability value range is 0-1. **Figure 2** describes the optimization results in the form of a 2D contour. *Contour* is a two-dimensional response image that was presented using a predictive model for PS, PDI, ZP, pH, spreadability, and AT response values. The contour graph shows the desirability value of 0.801, which is the closest value to 1 compared to the other points. **Figure 3** shows the projection in the form of a 3D surface; the low area shows low desirability, while the high area shows high desirability and is getting closer to 1. At this stage, the software predicts the response values shown in **Table 4**. Three confirmation runs need to be performed to validate optimization [61]. The optimization model and estimates are validated by the

observed optimized Negs, which show an acceptable variation from the predicted values (**Table 4**). We tested the optimized Negs' physical properties for further investigation, such as organoleptic, homogeneity, freeze-thaw, viscosity, and flow properties.

Table 4. Optimized TEO-loaded Negs' actual and predicted values for each response.

Responses	Predicted values	Actual value[a]	Error[b] (%)
Y1 (nm)	180.2	182.3 ± 5.5	1.165
Y2	0.250	0.242 ± 0.003	-3.200
Y3 (mV)	56.30	57.23 ± 2.91	1.652
Y4	4.50	4.51 ± 0.02	0.222
Y5 (cm)	6.07	6.0 ± 0.2	-1.153
Y6 (s)	6.98	6.45 ± 0.19	-7.593

a Data listed is the mean ± standart deviation, n = 3
b Error (%) = [(Actual value – Predicted value)/Predicted value] * 100%

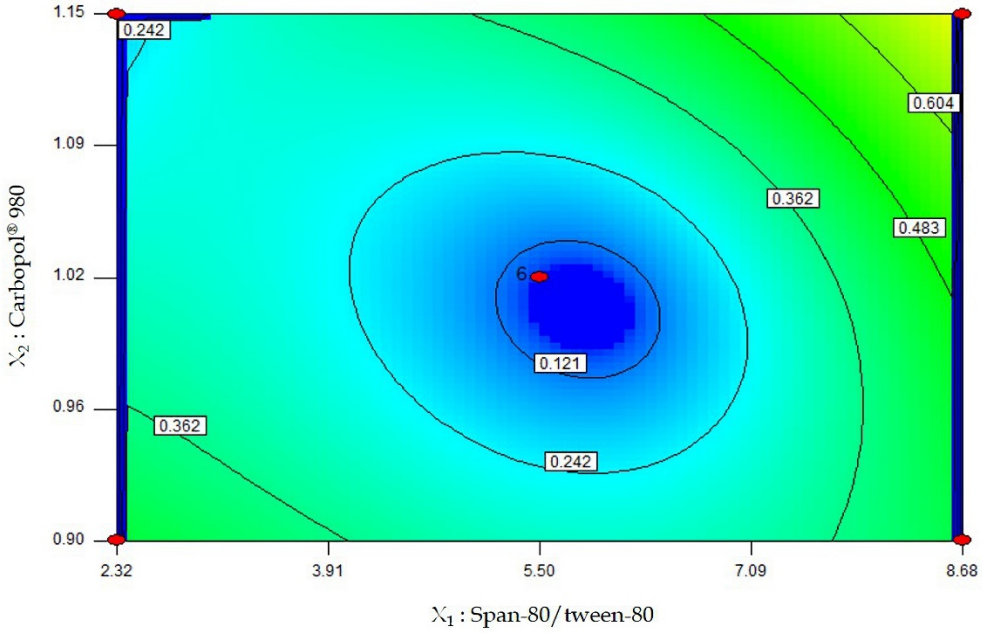

Figure 3. Contour plot desirability value of optimal formulation.

2.5. Evaluation of TEO-loaded Negs

Nanoemulsion systems can cover oily drugs' bitter or unpleasant taste [62]. The organoleptic results of TEO-loaded Negs have a less distinctive turmeric odor, which is white and semisolid (**Table 5**). That is due to the drug entrainment of oil with the oil phase effectively preventing evaporation and masking its specific odor [63]. The homogeneity test results of the optimum TEO-loaded Negs formulation showed a homogeneous preparation, as evidenced by the absence of coarse grains. This homogeneity was correlated with the optimal formulation of PS and PDI of 182.3 ± 5.5 and 0.242 ± 0.003, respectively. The low PDI indicates uniformity or homogeneous dispersion of globules Negs [64]. In addition, the small size of the globule (±200 nm) is not included in the coarse dispersion [41].

Table 5. Additional evaluation on TEO-loaded Negs with an optimal formulation.

Evaluation	Result
Organoleptic	Color: White; Odor: typical turmeric
Homogeneity	Homogeneous
Freeze-Thaw	Cycles 0-6, no separation occurs
Viscosity[a]	32240 ± 2257.7 cP

a Data listed is the mean ± standart deviation, n = 3

The thermodynamic stability test of the system was carried out using a freeze-thaw cycle to identify the presence of metastable Negs in the optimal formulation. It aims to see the separation of the water and oil phases due to the influence of extreme temperatures [65]. The thermodynamic stability of any system is determined by the change in free energy between the system and its surroundings [66]. The test results on the optimum formula for six cycles showed promising results; namely, there was no separation. This stability was correlated with the ZP of the optimal formulation of 57.23 ± 2.91 mV. The surface charge's magnitude was directly related to the stability of any Negs. It is evidenced by the high repulsive force between the Negs globules preventing coalescence, which was characterized by the absence of phase separation [67]. Similar results were found in the Negs study containing thymoquinone, which had ZPs between −26.7 and −30.6 mV [66].

The pH conditions indirectly affect the viscosity indicated by Negs because they influence the swelling ability of Carbopol® 980. This excipient is a gel former and a thickener [52]. It plays an essential role in the viscosity of Negs. Carbopol is dispersed in water to form an acidic colloidal solution with a low viscosity. Neutralizing with triethanolamine increases Negs' viscosity because a stable water-soluble gel was formed [50]. Viscosity was carried out with #7 spindle (Brookfield digital RV DV-E) at 50 rpm of 32240 ± 2257.7 cP, indicating significantly high viscosity on Negs with pH 4.5. The magnitude of the viscosity is correlated with AT and spreadability. Viscosity is inversely proportional to spreadability [52]. In contrast, the AT is directly proportional to the viscosity. A high-viscosity system will form stronger interfacial interactions and increase intermolecular interactions in the polymer network, increasing cohesion, adhesion strength, and AT [54].

Determining the rheology of a semisolid preparation is essential for controlling the consistency required to ensure the performance and formulation durability and to describe the mechanical (flow properties) system [68]. The rheological study was conducted in the shear rate range of 6.81-40.86 s^{-1} at 25°C. The consistency index equals the apparent viscosity at a shear rate of 1 s^{-1}. The consistency index measured on TEO-loaded Negs was 155.67 cP and n = 0.22. The flow index measures the system's deviation from Newtonian behavior (n = 1). A value of n > 1 indicates dilatation or shear thickening flow, and n < 1 indicates pseudoplastic or shear thinning. The flow index typically lowers the thicker the base. Negs produce a 0.22 flow index, which implies pseudoplastic flow behavior. A colloidal network structure aligned with the shear direction and decreases viscosity as the shear rate increases have led to this pseudo-plasticity. The developed system will require a specific force to discharge [69]. The results of the flow properties test showed that the optimal formula made was a pseudoplastic thixotropic flow type (**Figure 4**). *Thixotropic* is a flow property expected in pharmaceutical preparations because it has high consistency in the container but can be poured and dispersed easily [70].

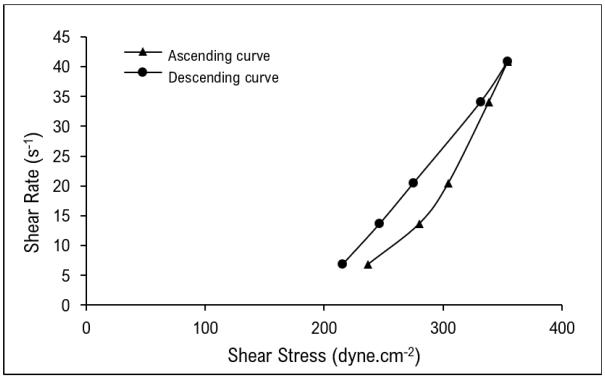

Figure 4. Optimal formulation flow properties.

3. CONCLUSION

Based on the results of the CCD-RSM analysis, the optimum span-80/tween-80 as an emulsifier is 8.68%, and Carbopol® 980 as a gel former was 1.18%. The resulting response is a PS of 182.3 nm, PDI 0.242, ZP 57.23 mV, pH 4.51, AT 6.45 seconds, and spreadability of 6 cm. Optimized formulation viscosity is 32240 cP with pseudoplastic thixotropic flow properties. Thus, the developed TEO-Negs can be a potential delivery system and a promising suitable approach for topical preparations.

4. MATERIALS AND METHODS

4.1. Materials

TEO (Curcuma longa) was purchased from Darjeeling Sembrani Aroma (Indonesia), sorbilene O E/P from Lamberti (Italy), span-80 from Croda (Singapura), propylene glycol from Dow Chemical Pacific (Singapura), Carbopol® 980 NF from Lubrizol AM (Cleveland), nipagin M from Clariant Produkte (Deutschland), propylparaben from Alpha Chemika (India), triethanolamine from Dow Chemical Pacific (Switzerland), and 1.1-diphenyl-2-picrylhydrazyl (DPPH) from Smart-Lab (Indonesia).

4.2. Methods

4.2.1. Identification of TEO

Organoleptic tests include observing form, color, and odor. Phenolic identification was carried out by adding one drop of 5% $FeCl_3$ to a 1 ml sample. Dark green to black colors indicate phenolic compounds' presence [71]. Terpenoid testing was performed by adding Lieberman-Burchard reagent containing anhydrous acetic acid and concentrated sulfuric acid (3:1) into a 1 ml sample. Brownish or violet ring form indicates the presence of terpenoids [72]. Spectrophotometry was used to determine antioxidant activity with the DPPH method [5]. The calibration curve for the DPPH concentration against absorbance was made at a maximum wavelength of 516 nm. The absorbance was measured in a mixture of sample solution and DPPH with a particular concentration after 30-min of incubation in a dark room. IC_{50} was calculated from the inhibition percentage and absorbance.

4.2.2. Preparation of TEO-loaded Negs

TEO-loaded Negs were produced using a high-energy method, which used a mechanical device to produce a highly disruptive force to break up the water and oil phases to obtain nano-sized globules [18]. The oil phase (M1) was prepared by mixing span-80 with 5% turmeric oil using a magnetic stirrer (WiseStir Wisd) at 1,500 rpm for 20 min. A total of 0.18% methylparaben and 0.02% propylparaben dissolved in 15% propylene glycol (M2). Then, the distilled water was stirred with tween-80, and M2 was added gradually until homogeneous at 1,500 rpm for 20 min (M3). M1 was stirred with M3 until homogeneous at 1,500 rpm for 40 min to form a clear and transparent nanoemulsion, then let left for 24 hours. The gel base was prepared by mixing Carbopol® 980 NF with distilled water at 70°C and left for 24 hours. Then, gradually add 1% triethanolamine to form a gel mass. Nanoemulsion was added slowly into the gel base while homogenized using a homogenizer (AEG) at 2,000 rpm for 10 min.

4.2.3. Experimental Design

This study selects the CCD-RSM method to develop the TEO-loaded Negs formulation. For preliminary screening on PS, PDI, ZP, pH, AT, and spreadability, a 2-factor CCD-RSM at two levels (high and low) was used. Based on previous experiments and study literature, high and low variables were determined. The CCD of the statistical package Design-Expert® version 13 software (Stat-Ease Inc., Minneapolis, MN) was used to examine the influence of the specified independent variable on the response variable to obtain the optimal formulation for TEO-loaded Negs. CCD planned 14 experiments were done under controlled circumstances (**Table 3**). The independent variables were span-80/tween-80 (X_1) and Carbopol® 980 concentration (X_2). The observed response of the dependent variables was PS (Y_1), PDI (Y_2), ZP (Y_3), pH (Y_4), spreadability (Y_5), and AT (Y_6).

4.2.4. Determination of PS, PDI, and ZP of Negs

PS and PDI of Negs were assessed using the Delsa Max Pro Particle Size Analyzer LS 100Q (Beckman Coulter, USA) at 25°C utilizing the dynamic light scattering (DLS) method or photo correlation spectroscopy. For analysis, 1 ml of samples was dispersed in 9 ml aqua pro injection. Into the cuvette, 1 ml of suspension and 5 ml of aqua pro injection were added as a diluent, and the results were read on the instrument. All measurements were made at a scattering angle of 90°. ZP was determined by particle size analyzer through mobility and conductivity measurements. The temperature was set to 25°C, and the mean electric field was set to 16 V/cm [73]. The final result is the mean of each sample's three repeated measurements.

4.2.5. Determination of pH, Spreadability, and AT

pH was measured at a temperature of 25°C using a pH meter that had been previously calibrated with buffer solutions of pH 4 and 7. The calibration step was completed when the pH value indicated on the screen matched the correct pH value and was stable. Afterward, the electrode was dipped in Negs and recorded the value shown on the screen [74]. Spreadability was measured by adding 0.5 g of Negs in the center of a glass covered with another glass. The preparation diameter was measured longitudinally and transversely; for every minute added, 50 g was to a total weight of 150 g [75]. Adhesion time determine by the single-lap shear test method [54]. A-0.5 g of Negs was placed on a slide, then covered with another slide, and given a load of 1 kg for 3 min. The glass object was mounted on the test apparatus, and 80 g of the load was released until both glass objects were released, and the time was recorded [75].

4.2.6. Organoleptic Observation and Homogeneity Test

Negs were placed in a glass object and directly observed for color, smell, and shape [76]. A-0.1 g Negs were spread over the slide, and homogeneity was observed. Test preparation is declared homogeneous if no coarse grains exist [77].

4.2.7. Viscosity and Rheological Flow

Viscosity and rheology were determined with a Brookfield RV DV-E Viscometer with appropriate spindle and speed. A-500 ml of Negs were put into a beaker glass; the spindle was installed, and the measured value was recorded as viscosity Negs. In this study, the spindle used spindle no. 7. Flow properties were determined by measuring the viscosity using a right spindle from low to high rotational speed and vice versa [74]. Flow index and consistency index are determined from the power law equation:

$$\tau = K\, r^n$$

where τ is the shear stress, K is the consistency index, r is the shear rate, and n is the flow index.
Taking logs on both sides,

$$\log \tau = \log K + n \log r$$

So, from the log, shear stress Vs. Log shear rate plot, the plot slope was used as the flow index and the antilog of the Y-intercept as the consistency index [69].

4.2.8. Freeze-thaw Test

Negs were stored at 4 ± 2 °C, then transferred to 40 ± 2 °C for 48 hours (1-cycle), then repeated for 6-cycles. Phase separation was observed in each cycle [74].

4.2.9. Statistical Analysis

The Design-Expert® version 13 software was used to conduct the statistical study (Stat-Ease Inc., Minneapolis, MN). Analysis was done at a sig—$p < 0.05$ and $p < 0.01$ after three times of each measurement.

Acknowledgments: This research was supported by a grant (Research of Science Development 275/F.03.07/2022) from Universitas Muhammadiyah Prof. DR. HAMKA, Indonesia.

Author contributions: Concept – N.N., A.A., F.Z; Design – A.A., F.Z.; Supervision – N.N., A.A.; Resources – N.N., F.Z.; Materials – F.Z.; Data Collection and Processing – A.A., F.Z.; Analysis and Interpretation – N.N., A.A., F.Z.; Literature Search – N.N., F.Z.; Writing – N.N.; Critical Reviews – A.A., F.Z.

Conflict of interest statement: The authors declare no conflict of interest.

REFERENCES

[1] Rohman A, Widodo H, Lukitaningsih E, Rafi M, Nurrulhidayah AF, Windarsih A. Review on *in-vitro* antioxidant activities of Curcuma species commonly used as. Food Res. 2020;4(2):286–293. https://doi.org/10.26656/fr.2017.4(2).163.

[2] Liju VB, Jeena K, Kuttan R. An evaluation of antioxidant, anti-inflammatory, and antinociceptive activities of essential oil from *Curcuma longa*. L. Indian J Pharmacol. 2011;43(5):526–531. https://doi.org/10.4103/0253-7613.84961

[3] Devkota L, Rajbhandari M. Composition of essential oils in turmeric rhizome. Nepal J Sci Technol. 2016;16(1):87–94. https://doi.org/10.3126/njst.v16i1.14361

[4] Guimarãesa AF, Vinhas ACA, Gomes, Angélica Ferraz Souza LH, Krepsky PB. Essential oil of *Curcuma longa* L.

rhizomes chemical composition, yield variation and stability. Quim Nov. 2020;43(7):909–913. https://doi.org/10.21577/0100-4042.20170547

[5] Islamadina R, Can A, Rohman A. Chemometrics application for grouping and determinating volatile compound which related to antioxidant activity of turmeric essential oil (*Curcuma longa* L). J Food Pharm Sci. 2020;8(2):225-239 https://doi.org/10.22146/jfps.658

[6] Dosoky NS, Setzer WN. Chemical composition and biological activities of essential oils of curcuma species. Nutrients. 2018;10(9):10–17. https://doi.org/10.3390/nu10091196

[7] Jankasem M, Wuthi-udomlert M, Gritsanapan W. Antidermatophytic properties of ar -turmerone, turmeric oil, and *Curcuma longa* preparations. ISRN Dermatol. 2013;2013(April 2009):1–3. https://doi.org/10.1155/2013/250597

[8] Mishra R, Gupta AK, Kumar A, Lal RK, Saikia D, Chanotiya CS. Genetic diversity, essential oil composition, and *in-vitro* antioxidant and antimicrobial activity of *Curcuma longa* L. germplasm collections. J Appl Res Med Aromat Plants. 2018;10(December 2017):75–84. https://doi.org/10.1016/j.jarmap.2018.06.003

[9] Sharifi-Rad J, Rayess YE, Rizk AA, Sadaka C, Zgheib R, Zam W, Sestito S, Rapposelli S, Neffe-Skocińska K, Zielińska D, Salehi B, Setzer WN, Dosoky NS, Taheri Y, El Beyrouthy M, Martorell M, Ostrander EA, Suleria HAR, Cho WC, Maroyi A, Martins N. Turmeric and Its major compound curcumin on health: Bioactive effects and safety profiles for food, pharmaceutical, biotechnological and medicinal applications. Front Pharmacol. 2020;11:01021. https://doi.org/10.3389/fphar.2020.01021

[10] Vera JMV, Dueñas-Rivadeneira AA, Díaz JMR, Radice M. Phytochemical characterization of the ethanolic extract, antioxidant activity, phenolic content and toxicity of the essential oil of *Curcuma longa* L. Rev la Fac Agron (LUZ). 2022;39(1) e223906. https://doi.org/10.47280/RevFacAgron(LUZ).v39.n1.06

[11] Ali MS, Alam MS, Imam F, Siddiqui MR. Topical nanoemulsion of turmeric oil for psoriasis: Characterization, *ex-vivo* and *in-vivo* assessment. Int J Drug Deliv. 2012;4(2):184–197. https://doi.org/10.5138/ijdd.v4i2.575

[12] Meng F-C, Zhou Y-Q, Ren D, Wang R, Wang C, Lin L-G, Zhang X-Q, Ye W-C, Zhang Q-W. Turmeric: A review of ıts chemical composition, quality control, bioactivity, and pharmaceutical application. Natural and Artificial Flavoring Agents and Food Dyes. Elsevier Inc.; 2018. 299–350. https://doi.org/10.1016/B978-0-12-811518-3.00010-7

[13] Ibáñez MD, Blázquez MA. Curcuma longa L. rhizome essential oil from extraction to its agri-food applications. A review. Plants. 2021;10(1):1–31. https://doi.org/10.3390/plants10010044

[14] Yan W, Bowen WD, Hopson R, Mathew AE, Jacob JN. Biological studies of turmeric oil, part 2: Isolation and characterization of turmeric oil components; cytotoxic activity against pancreatic cancer cells. Nat Prod Commun. 2013;8(6):811–814. https://doi.org/10.1177/1934578x1300800633

[15] Sarojini S, Sundar K, Anjali CH, Ravindran A. Formation and stability of oil-in-water nano emulsion containing turmeric oil. BTAIJ. 2014;9(4):171–177

[16] Vishwakarma AK, Maurya OP, Nimisha, Srivastava D. Formulation and evaluation of transdermal patch containing turmeric oil. Int J Pharm Pharm Sci. 2012;4(SUPPL. 5):358–361.

[17] Kirtane AR, Karavasili C, Wahane A, Freitas D, Booz K, Le DTH, Hua T, Scala S, Lopes A, Hess K, Collins J, Tamang S, Ishida K, Kuosmanen JLP, Rajesh NU, Phan NV, Li J, Krogmann A, Lennerz JK, Hayward A, Langer R, Traverso G. Development of oil-based gels as versatile drug delivery systems for pediatric applications. Sci Adv. 2022;8(21) 27;8(21):eabm8478. https://doi.org/10.1126/sciadv.abm8478

[18] Sengupta P, Chatterjee B. Potential and future scope of nanoemulgel formulation for topical delivery of lipophilic drugs. Int J Pharm. 2017;526(1–2):353–365. https://doi.org/10.1016/j.ijpharm.2017.04.068

[19] Eid AM, El-Enshasy HA, Aziz R, Elmarzugi NA. Preparation, characterization and anti-inflammatory activity of Swietenia macrophylla nanoemulgel. J Nanomedicine Nanotechnol. 2014;5(2):190. https://doi.org/10.4172/2157-7439.1000190

[20] Khurana S, Jain NK, Bedi PMS. Nanoemulsion based gel for transdermal delivery of meloxicam: Physico-chemical, mechanistic investigation. Life Sci. 2013;92(6–7):383–392. https://doi.org/10.1016/j.lfs.2013.01.005

[21] Baibhav J, Gurpreet S, Rana A, Seema S, Vikas S. Emulgel: A comprehensive review on the recent advances in topical drug delivery. Int Res J Pharm. 2011;2(11):66–70.

[22] Sultana N, Akhtar J, Badruddeen, Khan MI, Ahmad U, Arif M, et al. Drug Development Life Cycle. Akhtar J, Badruddeen, Ahmad M, Irfan Khan M. (Eds.). IntechOpen, 2022. https://doi.org/10.5772/intechopen.96842

[23] Eswaraiah S, Swetha K, Lohita M, Preethi PJ, Priyanka B, Reddy KK. Emulgel : Review on novel approach to topical drug delivery. Asian J Pharm Res. 2014;4(1):4–11.

[24] Dhawan B, Aggarwal G, Harikumar S. Enhanced transdermal permeability of piroxicam through novel nanoemulgel formulation. Int J Pharm Investig. 2014;4(2):65–76. https://doi.org/10.4103/2230-973x.133053

[25] Dev A, Chodankar R, Shelke O. Emulgels : A novel topical drug delivery system. Pharm Biol Eval. 2015;2(4):64–75.

[26] ICH. ICH Guideline Q9 on Quality Risk Management. Vol. 44, Regulatory ICH. 2005. 1–20 p.

[27] Abdallah MH, Elsewedy HS, Abulila AS, Almansour K, Unissa R, Elghamry HA, Soliman MS. Quality by design for optimizing a novel liposomal jojoba oil-based emulgel to ameliorate the anti-inflammatory effect of brucine. Gels. 2021;7(4):219. https://doi.org/10.3390/gels7040219

[28] Sindi AM, Hosny KM, Alharbi WS. Lyophilized composite loaded with meloxicam-peppermint oil nanoemulsion for periodontal pain. Polymers (Basel). 2021;13(14):2317. https://doi.org/10.3390/polym13142317

[29] Yalçinkaya SE, Yildiz N, Ak MS, Çalimli A. Preparation of polystyrene/montmorillonite nanocomposites: Optimization by response surface methodology (RSM). Turk J Chem. 2010;34(4):581–592. https://doi.org/10.3906/kim-0908-235

[30] Klangmanee K, Athipornchai A. A rapid phytochemical screening of the effective phenolic antioxidant agents using

$FeCl_3$ reagent. J Pharm Sci Res. 2019;11(10):3475–3480.
[31] Orellana-Paucar AM, Machado-Orellana MG. Pharmacological profile, bioactivities, and safety of turmeric oil. Molecules. 2022;27(16):5055. https://doi.org/10.3390/molecules27165055
[32] Kusmardiyani S, Novita G, Fidrianny I. Antioxidant activities from various extracts of different parts of kelakai (Stenochlaena palustris) grown in central Kalimantan - Indonesia. Asian J Pharm Clin Res. 2016;9:215–219. https://doi.org/10.22159/ajpcr.2016.v9s2.13630
[33] Avanco GB, Ferreira FD, Bonfim NS, Souza Rodrigues dos Santos PA, Peralta R, Brugnari T, Mallmann CA, Alves deAbreu Filho B, Graton Mikcha JM, Machinski Jr M. *Curcuma longa* L. essential oil composition, antioxidant effect, and effect on *Fusarium verticillioides* and fumonisin production. Food Control. 2017;73:806–813. https://doi.org/10.1016/j.foodcont.2016.09.032
[34] Priya R, Prathapan A, Raghu KG, Menon AN. Chemical composition and *in-vitro* antioxidative potential of essential oil isolated from *Curcuma longa* L. leaves. Asian Pac J Trop Biomed. 2012;2(2 SUPPL.):S695–699. https://doi.org/10.1016/S2221-1691(12)60298-6
[35] Pino JA, Fon-Fay FM, Pérez JC, Falco AS, Hernández I, Rodeiro I, Fernandez MD. Chemical composition and biological activities of essential oil from turmeric (*Curcuma longa* L.) rhizomes grown in Amazonian Ecuador. CENIC Ciene Quím. 2018;49:1–8.
[36] Setya S, Madaan T, Tariq M, Razdan BK, Talegaonkar S. Appraisal of transdermal water-in-oil nanoemulgel of selegiline HCI for the effective management of parkinson's disease: Pharmacodynamic, pharmacokinetic, and biochemical ınvestigations. AAPS PharmSciTech. 2018;19(2):573–589. https://doi.org/10.1208/s12249-017-0868-0
[37] Chang WC, Hu YT, Huang Q, Hsieh SC, Ting Y. Development of a topical applied functional food formulation: Adlay bran oil nanoemulgel. LWT 2020;117:108619. https://doi.org/10.1016/j.lwt.2019.108619
[38] Ye Q, Li J, Li T, Ruan J, Wang H, Wang F, Zhang X. Development and evaluation of puerarin-loaded controlled release nanostructured lipid carries by central composite design. Drug Dev Ind Pharm. 2021;47(1):113–125. https://doi.org/10.1080/03639045.2020.1862170
[39] Shehata TM, Elnahas HM, Elsewedy HS. Development, characterization and optimization of the anti-ınflammatory ınfluence of meloxicam loaded into a eucalyptus oil-based nanoemulgel. Gels. 2022;8(5):262. https://doi.org/10.3390/gels8050262
[40] How CW, Rasedee A, Abbasalipourkabir R. Characterization and cytotoxicity of nanostructured lipid carriers formulated with olive oil, hydrogenated palm oil, and polysorbate 80. IEEE Trans Nanobioscience. 2013;12(2):72–78. https://doi.org/10.1109/tnb.2012.2232937
[41] Chuacharoen T, Prasongsuk S, Sabliov CM. Effect of surfactant concentrations on physicochemical properties and functionality of curcumin nanoemulsions under conditions relevant to commercial utilization. Molecules. 2019;24(15):2744. https://doi.org/10.3390/molecules24152744
[42] Sarheed O, Dibi M, Ramesh KVRNS. Studies on the effect of oil and surfactant on the formation of alginate-based O/W lidocaine nanocarriers using nanoemulsion template. Pharmaceutics. 2020;12(12):1223. https://doi.org/10.3390/pharmaceutics12121223
[43] McClements DJ. Food Emulsions: Principles, Practices, and Techniques. Third Edit. New York: CRC Press; 2016, pp.719.
[44] Danaei M, Dehghankhold M, Ataei S, Hasanzadeh Davarani F, Javanmard R, Dokhani A, Khorasani S, Mozafari MR. Impact of particle size and polydispersity index on the clinical applications of lipidic nanocarrier systems. Pharmaceutics. 2018;10(2):57. https://doi.org/10.3390/pharmaceutics10020057
[45] Choi AJ, Kim CJ, Cho YJ, Hwang JK, Kim CT. Characterization of capsaicin-loaded nanoemulsions stabilized with alginate and chitosan by self-assembly. Food Bioprocess Technol. 2011;4:1119–1126. https://doi.org/10.1007/s11947-011-0568-9
[46] Sinha P, Srivastava S, Mishra N, Singh DK, Luqman S, Chanda D, Yadav NP. Development, optimization, and characterization of a novel tea tree oil nanogel using response surface methodology. Drug Dev Ind Pharm. 2016;42(9):1434–1445. https://doi.org/10.3109/03639045.2016.1141931
[47] Honary S, Zahir F. Effect of zeta potential on the properties of nano-drug delivery systems - a review (part 1). Trop J Pharm Res. 2013;12(2):255–264. https://doi.org/10.4314/tjpr.v12i2.19
[48] Gurpreet K, Singh SK. Review of nanoemulsion formulation and characterization techniques. Indian J Pharm Sci. 2018;80(5):781–789. https://doi.org/10.4172/pharmaceutical-sciences.1000422
[49] Dias IP, Barbieri SF, Fetzer DEL, Corazza ML, Silveira JLM. Effects of pressurized hot water extraction on the yield and chemical characterization of pectins from *Campomanesia xanthocarpa* Berg fruits. Int J Biol Macromol. 2020;146:431–443. https://doi.org/10.1016/j.ijbiomac.2019.12.261
[50] Kulkarni VS, Shaw C. Use of polymers and thickeners in semisolid and liquid formulations. Essent Chem Formul Semisolid Liq Dosages. 2016;43–69. https://doi.org/10.1016/b978-0-12-801024-2.00005-4
[51] Corporation TL. Product Specification Carbopol 980 NF Polymer. Cleveland; 2017.
[52] Nurman S, Yulia R, Irmayanti, Noor E, Sunarti TC. The optimization of gel preparations using the active compounds of arabica coffee ground nanoparticles. Sci Pharm. 2019;87(4):32. https://doi.org/10.3390/scipharm87040032
[53] Kurniawan MF, Sugihartini N, Yuwono T. Iritation properties and evaluation of physical properties emulgel of clove oil using simplex lattice design methods. Farmasains J Ilm Ilmu Kefarmasian. 2018;5(1):1–8. https://doi.org/10.22236/farmasains.v5i1.1111
[54] Sun Z, Li Z, Qu K, Zhang Z, Niu Y, Xu W, Ren C. A review on recent advances in gel adhesion and their potential applications. J Mol Liq. 2021;325:115254. https://doi.org/10.1016/j.molliq.2020.115254

[55] Gupta NV, Natasha S, Getyala A, Bhat RS. Bioadhesive vaginal tablets containing spray dried microspheres loaded with clotrimazole for treatment of vaginal Candidiasis. Acta Pharm. 2013;63(3):359–372. https://doi.org/10.2478/acph-2013-0027
[56] Abramowitch S, Easley D. Introduction to Classical Mechanics. Biomechanics of the Female Pelvic Floor. Elsevier Inc.; 2016, pp. 89–107. https://doi.org/10.1016/B978-0-12-803228-2.00004-0
[57] Sari DK, Sugihartini N, Yuwono T. Irritation test and physical properties evaluation of essential oils clove (Syzigium aromaticum) in emulgel. Pharmaciana. 2015;5(2):115–120. https://doi.org/10.12928/pharmaciana.v5i2.2493
[58] Cevher E, Sensoy D, Taha MAM, Araman A. Effect of thiolated polymers to textural and mucoadhesive properties of vaginal gel formulations prepared with polycarbophil and chitosan. AAPS PharmSciTech. 2008;9(3):953–965. https://doi.org/10.1208/s12249-008-9132-y
[59] Pande V, Patel S, Patil V, Sonawane R. Design expert assisted formulation of topical bioadhesive gel of sertaconazole nitrate. Adv Pharm Bull. 2014;4(2):121–130. https://doi.org/10.5681/apb.2014.019
[60] Badwaik LS, Prasad K, Deka SC. Optimization of extraction conditions by response surface methodology for preparing partially defatted peanut. Int Food Res J. 2012;19(1):341–346.
[61] Mohtashamian S, Boddohi S, Hosseinkhani S. Preparation and optimization of self-assembled chondroitin sulfate-nisin nanogel based on quality by design concept. Int J Biol Macromol. 2018;107:2730–2739. https://doi.org/10.1016/j.ijbiomac.2017.10.156
[62] Jaiswal M, Dudhe R, Sharma PK. Nanoemulsion: An advanced mode of drug delivery system. 3 Biotech. 2015;5(2):123–127. https://doi.org/10.1007/s13205-014-0214-0
[63] Wang X, Gu Y, He Y, Sang L, Dai Y, Wang D. Preparation and optimization formulation of zedoary turmeric oil nanoemulsion based thermo-sensitive gel for improved application in ophthalmology. J Drug Deliv Sci Technol. 2021;65:102682. https://doi.org/10.1016/j.jddst.2021.102682
[64] Begur M, Kumar Pai V, Gowda D V, Srivastava A, Raghundan H V, Shinde CG, et al. Enhanced permeability of Cyclosporine from a transdermally applied nanoemulgel. Der Pharm Sin. 2015;6(2):69–79.
[65] Yuliani SH, Hartini M, Pudyastuti B, Istyastono EP. Comparison of physical stability properties of pomegranate seed oil nanoemulsion dosage forms with long-chain triglyceride and medium-chain triglyceride as the oil phase. Tradit Med J. 2016;21(2):93–98. https://doi.org/10.22146/tradmedj.12823
[66] Algahtani MS, Ahmad MZ, Shaikh IA, Abdel-Wahab BA, Nourein IH, Ahmad J. Thymoquinone loaded topical nanoemulgel for wound healing: Formulation design and *in-vivo* evaluation. Molecules. 2021;26(13):3863. https://doi.org/10.3390/molecules26133863
[67] Ahmad J, Mir SR, Kohli K, Amin S. Effect of oil and co-surfactant on the formation of Solutol HS 15 based colloidal drug carrier by Box-Behnken statistical design. Colloids Surfaces A Physicochem Eng Asp. 2014;453(1):68–77. https://doi.org/10.1016/j.colsurfa.2014.04.008
[68] Eid AM, Hawash M. Biological evaluation of safrole oil and safrole oil Nanoemulgel as antioxidant, antidiabetic, antibacterial, antifungal and anticancer. BMC Complement Med Ther. 2021;21(1):159. https://doi.org/10.1186/s12906-021-03324-z
[69] Arora R, Aggarwal G, Harikumar SL, Kaur K. Nanoemulsion based hydrogel for enhanced transdermal delivery of ketoprofen. Adv Pharm. 2014;2014:468456. https://doi.org/10.1155/2014/468456
[70] Sinko PJ, Singh Y, editors. Martin's physical pharmacy and pharmaceutical sciences, 6th edt. Philadelphia: Wolter Kluwer Health; 2011.
[71] Rahimah SB, Djunaedi DD, Soeroto AY, Bisri T. The phytochemical screening, total phenolic contents and antioxidant activities *in-vitro* of white oyster mushroom (*Pleurotus ostreatus*) preparations. Open Access Maced J Med Sci. 2019;7(15):2404–2412. https://doi.org/10.3889/oamjms.2019.741
[72] Farabi K, Harneti D, Darwati, Mayanti T, Nurlelasari, Maharani R, Sari AP, Herlina T, Hidayat AT, Supratman U, Fajriah S, Azmi MN, Shiono Y. Dammarane-type triterpenoid from the stem bark of *Aglaia elliptica* (Meliaceae) and ıts cytotoxic activities. Molecules. 2022;27(19):6757. https://doi.org/10.3390/molecules27196757
[73] Elsheikh MA, Elnaggar YSR, Hamdy DA, Abdallah OY. Novel cremochylomicrons for improved oral bioavailability of the antineoplastic phytomedicine berberine chloride: Optimization and pharmacokinetics. Int J Pharm. 2018;535(1–2):316–324. https://doi.org/10.1016/j.ijpharm.2017.11.023
[74] Nursal FK, Nining, Rahmah AS. Formulation and development of grape seed oil (*Vitis vinifera* L) emulgel peel-off mask using gelling agent hydroxy propyl methyl cellulose (HPMC). IOP Conf Ser Earth Environ Sci. 2021;755(1):012046. https://doi.org/10.1088/1755-1315/755/1/012046
[75] Irianto IDK, Purwanto P, Mardan MT. Antibacterial activity and physical evaluation of *Piper betle* L. Decoction gel as an alternative treatment for mastitis. Majalah Farmaseutik. 2020;16(2):202–210. https://doi.org/10.22146/farmaseutik.v16i2.53793
[76] Elfiyani R, Amalia A, Pratama SY. Effect of using the combination of tween 80 and ethanol on the forming and physical stability of microemulsion of eucalyptus oil as antibacterial. J Young Pharm. 2017;9(2):230–233. https://doi.org/10.5530/jyp.2017
[77] Yati K, Jufri M, Gozan M, Dwita LP. The effect of hidroxy propyl methyl cellulose (HPMC) concentration variation on physical stability of tobacco (*Nicotiana tabaccum* l.) extract gel and ıts activity against *Streptococcus mutans*. Pharm Sci Res. 2018;5(3):133–141. https://doi.org/10.7454/psr.v5i3.4146